Measurement of particle size distribution in multilayered skin phantoms using polarized light spectroscopy

Matthew Bartlett and Huabei Jiang*
Department of Physics and Astronomy, Clemson University, Clemson, South Carolina 29634
(Received 14 September 2001; published 19 February 2002)

We report on the ability to use polarized light to measure the particle size distribution of thin layers of polystyrene microspheres on top of a solid Intralipid phantom. The optical properties of each layer were adjusted to match the absorption and scattering properties of the epidermis (polystyrene layer) and dermis (Intralipid layer). Polarized light was used to discriminate between light scattered from the top layer of polystyrene and the lower layer of Intralipid. In this paper we also study the effect of the thickness of the top layer on the ability to reconstruct the polystyrene size distribution.

DOI: 10.1103/PhysRevE.65.031906 PACS number(s): 87.64.Cc, 42.25.Ja, 42.62.Be

I. INTRODUCTION

The *in vivo* measurement of the cell or nuclear size distribution of thin tissue layers is important for the early diagnosis of skin cancer and dysplasia. Currently over half of all cancers are skin cancers and as many as 10 000 people die every year from some form of skin cancer [1]. Early diagnosis remains crucial for effective treatment of skin cancer. The current method for detecting skin cancer involves repeated visual screenings followed by biopsy of any suspected areas. This method suffers from dependence upon subjective visual observations and painful biopsies. An estimated 51 400 people will develop melanoma this year, of which 7800 will die [1]. This death rate is primarily due to a lack of repeated screening. Improved diagnostic methods, which are noninvasive and, therefore, nonpainful, could significantly improve the screening level of people at heightened risk of skin cancer.

The skin consists of two primary layers that include the epidermis, top layer, and dermis, bottom layer. Under the dermis is subcutaneous tissue, or hypodermis, which consists of connective tissue, fibroblasts, and fat cells among other components. The epidermis primarily consists of cells called keratinocytes. These cells develop in the basal layer of the skin at the bottom of the epidermis. As they migrate to the surface, they flatten and cornify—harden—sealing the skin [2]. The epidermis also includes melanocytes located near the base of the epidermis. These cells secrete the pigment melanin that protects the skin from ultraviolet radiation. The dermis can vary in thickness from 1 to 4 mm. It is primarily made up of fibrous connective tissue such as collagen. The dermis also contains the hair follicles, sweat glands, blood vessels, and nerves making it a very complex optical tissue.

There are three basic types of skin cancer that include basal carcinoma, squamous carcinoma, and malignant melanoma. All three of these skin cancers originate in the epidermal layer with malignant melanoma being the most dangerous due to its tendency to metastasize, spread. Melanoma can be particularly difficult to diagnose because of its similarity to dysplastic nevi often referred to as moles. Patients with dysplastic nevi present a challenge to health professionals because these patients are not only at high risk of developing melanoma, but the early visual indications of cancer are often masked by the mole. Because cancer cells undergo rapid cell division, there is often a significant shift in the nuclear size and cell size that is not present in noncancerous cells [3]. If the cell size distribution could be monitored *in vivo*, a shift in the mean or standard deviation could indicate the presence of cancer. Polarized light measurements may provide a way to monitor the subsurface condition of moles, giving early warning of abnormal cellular activity. Repeated checkup would provide a base line cell size distribution that could be monitored for abnormal shifts.

Recent studies have shown [4,5] that the *in vivo* measurement of particle size distribution using continuous-wave light is possible for semi-infinite, homogeneous samples. These conditions are not remotely met with skin that is thin, multilayered, and relatively complex. The need for a semi-infinite sample can be overcome by changing from a multi-scattering, diffusion based model to a single scattering model based on polarized light. There has been recent interest in using polarized light to monitor thin layers of tissue. These methods have varied from enhancing video images using polarized light to using scattered light to directly measure the particle size distribution (PSD) of a sample.

As early as 1997 Demos and Alfano [6] showed that polarized light combined with time resolved techniques could be used to obtain enhanced images of different layers of the skin. These researchers were able to discriminate between light scattered from the very top layer of the skin and light scattered from deeper layers. They shined parallel polarized light onto a sample and used an analyzer to measure both parallel and perpendicular light. Light from the top layer tends to maintain its polarization while light from deeper layers looses its polarization. They also used the wavelength dependence of the absorption of light to selectively image deeper layers of tissue *in vivo*.

Jacques, Roman, and Lee [7] used the differences in parallel and perpendicular light to enhance video images of tissue effected by cancer. They were able to significantly enhance the diagnosis of cancerous skin tissue by subtracting

*Corresponding author. FAX: 865-656-0805. Email address: hjiang@clemson.edu

light scattered from deeper tissues, represented by perpendicular polarized light.

Hielscher, Maurant, and Bigio [8] directed an incident beam of linear polarized light onto a sample and collected the diffuse backscattered light with parallel and perpendicular analyzers. They collected an image of the backscattered light and found distinctive spatially dependent patterns in the scattered light that were unique for both parallel and perpendicular light. The pattern of the light was related to the particle size and optical properties of the sample. This study found a correlation between the angular dependence of the scattering and the particle's size.

The above studies image the area of interest but do not give extensive information about the size distributions of the sample. A recent study performed by Backman *et al.* [9] used perpendicular and parallel light to reconstruct the PSD of a thin layer of colon cells. Their method used polarization properties to isolate light scattered from the top layer. By comparing the measured single scattered light to the intensity spectrum predicted by Mie theory, the size distribution of the cells was determined. The results of this study show the significant difference in cellular size distribution between normal and tumor colon cells.

In this paper we use polarized light to measure the PSD in a thin top layer of tissue phantoms. An analyzer is used to discriminate between light scattered from the top layer and light that has been multiply scattered from the deeper, second layer. In this study we use polystyrene spheres to represent the epidermal layer and a solid Intralipid phantom as the dermal layer. Mie theory provides a powerful theoretical tool for predicting the wavelength dependent intensity of polarized light scattered from a particle. The theory is particularly simple when the particle is a sphere such as polystyrene. Cells are seldom entirely spherical, particularly skin cells that flatten and stiffen as they move to the surface. However, cells deeper in the epidermal layer tend to be more spherical. Since this area is where most skin cancers begin, we believe Mie scattering from spheres should be a reasonable approximation.

Although our method is most similar to that proposed by Backman *et al.*, we use a simpler model to reconstruct the PSD. By removing the requirement that the light be scattered directly backward, 180° from the incident, we simplify the experimental setup and the theoretical model. In our experiments we place a 30° angle between the incident and collecting fibers. Using our method we demonstrate the ability to reconstruct the PSD of three different diameter polystyrene samples mixed with water and India ink as an absorber. Since skin is very thin and can vary in thickness, we also show the effect that different thicknesses of the top layer have on the reconstructed size distribution. For each diameter sphere we placed three different thicknesses of polystyrene phantoms on top of an Intralipid phantom. These three thicknesses were chosen to match possible epidermal depths. To make the study more realistic we adjusted the optical properties of the phantoms to match the absorption and scattering of skin.

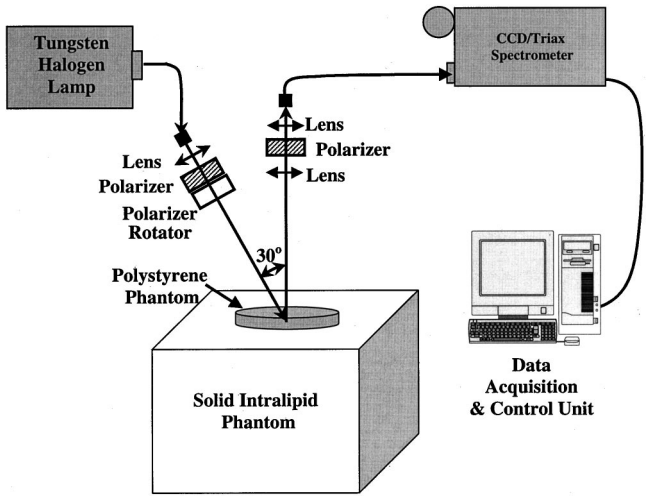

FIG. 1. The entire experimental setup including light source, polarizer, analyzer, sample, CCD/Triax spectrometer, and computer.

II. EXPERIMENT

Experiments were conducted with a charge-coupled-device- (CCD)- based continuous-wave system shown in Fig. 1. In this system light produced by 100-W tungsten halogen lamp was focused onto a 200-μm fiber optic cable that delivered the light to the sample. The light was directed through a collimating lens, a polarizer connected to a rotational device, and then through a focusing lens. The incident light focused to a 1.5-mm-diameter circular spot on the surface of the sample. The center of the incident beam was directed at the sample from an angle of 30° from the normal. After impinging on the sample, the light that scattered normal to the surface was collected by an analyzer. The analyzer was kept stationary and transmitted light polarized parallel to the scattering plane (defined by the direction of incident light and the collected light—normal to the sample surface). A collection lens then focused the light onto the tip of a 200-μm-diameter fiber optic cable connected to an ISA 3200 CCD spectrometer interfaced with a computer. The system measured the light intensity vs wavelength over a wavelength range from 540–810 nm.

The incident polarizer was connected to a hand operated rotational device that allowed us to rotate the polarizer by 90°. The collection polarizer was kept stationary throughout all the experiments. For each sample, we collected two sets of data, one with the incident polarizer set parallel to the collection polarizer, $\mathbf{I}_{\|}(\lambda)$, and the second with the incident polarizer set perpendicular to the collection polarizer, $\mathbf{I}_{\perp}(\lambda)$.

The samples consisted of three sets of polystyrene latex spheres with mean diameters of 0.75, 5.83, and 9.10 μm. For both the 0.75- and 5.83-μm spheres, deionized water was added to adjust the reduced scattering coefficient μ_s' to match the scattering of skin. For the 9.10-μm spheres, the sample was allowed to settle and excess water was decanted off. India ink was also added to the latex phantoms to make the absorption coefficient μ_a match that of the epidermis. The optical properties of the polystyrene phantoms were set such that $\mu_s' = 2.0/\text{mm}$ and $\mu_a = 2.46/\text{mm}$. The polystyrene phantoms were placed on top of an Intralipid solid phantom

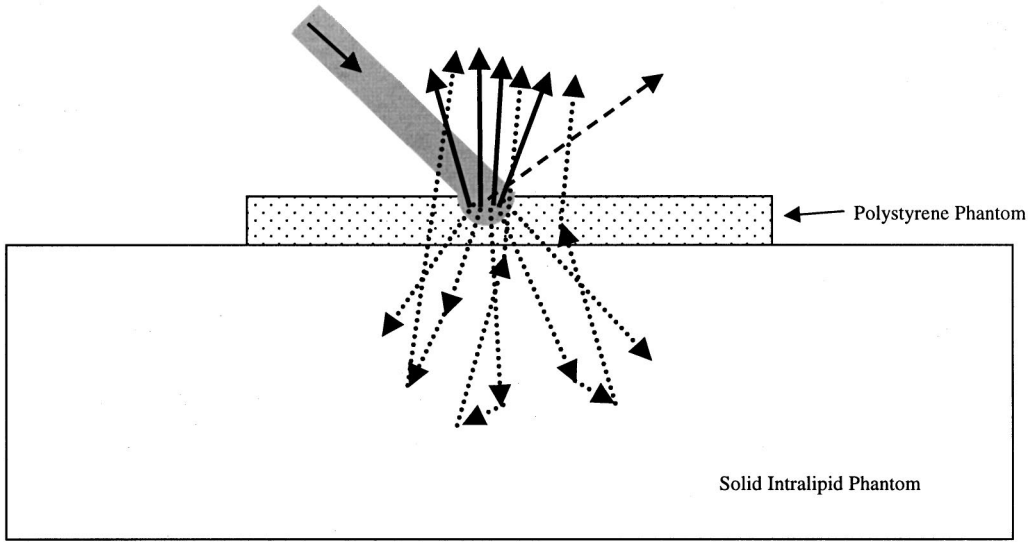

FIG. 2. Linear polarized light is incident from the left onto the polystyrene phantom. Some of the light undergoes specular reflectance from the surface (dashed line). Some of the incident light scatters from the top layer and maintains its polarization (solid black arrows). Some of the light travels deep into the sample and is either absorbed or scattered back to the surface as unpolarized light (dotted lines).

made from agar (a stiffening agent), distilled water, India ink, and 10% Intralipid. The optical properties of this phantom were adjusted such that $\mu_s' = 2.0/\text{mm}$ and $\mu_a = 0.03/\text{mm}$. These optical properties approximate the scattering and absorption of the epidermal and dermal layer of the skin at 650 nm [10,11].

For each diameter of polystyrene spheres, a 4-cm cube of Intralipid solid phantom was placed below the incident light. To simulate a thin layer of skin, a 12-μl drop of polystyrene phantom was placed onto the center of the solid phantom, see Fig. 1. This drop spread out in a uniform circle with a diameter that could be easily measured using a vernier caliper. Knowing the original volume and the area this drop covered allowed us to calculate the approximate polystyrene thickness. After waiting a few seconds for the drop area to become stable, a parallel and polarized measurement were taken. A second 12-μl drop was then added to the first to increase the sample depth, and the procedure repeated. Using this method we were able to obtain an average top layer thickness of between 50 and 179 μm. This thickness is comparable to the thickness of the epidermal layer of the skin that can very from 70 to 150 μm for thin skin and up to 600 μm for the hands and soles of the feet [12]. In order to remove the wavelength dependence of the polarizers, parallel and perpendicular measurements were taken on a standard diffuser and used to normalize the experimental measurements.

III. THEORY

Since most types of skin cancers begin in the epidermal layer and result in a significant shift in the nuclear size distribution of the cell, a method for monitoring the nuclear size distribution of this thin layer *in vivo* would be a useful diagnostic tool. Polarized light provides the means to monitor this thin top layer. Linear polarized light can be scattered multiple times in an optically dense medium before loosing its polarization [13,14]. Because of this, light that scatters from a thin layer maintains a significant percentage of its polarization. However, light that travels deeper into the sample tends to loose all its initial polarization before being scattered back to the surface.

In our method we use a polarizer connected to a rotational stage to divide the incident white light into two equal components of parallel $\mathbf{I}_{\parallel}\hat{\mathbf{e}}_i$ and perpendicular $\mathbf{I}_{\perp}\hat{\mathbf{e}}_i$—defined according to the scattering plane. Here $\mathbf{I}_{\parallel}^{i}$ means incident parallel intensity, $\hat{\mathbf{e}}_i$ indicates the direction of the incident beam, $\mathbf{I}_{\perp}^{i}$ means incident perpendicular intensity, and $\hat{\mathbf{e}}_c$ indicates the direction from the scattering event to the collector. When the parallel light strikes the sample, some of the light undergoes specular reflectance, but most of the light enters the sample. Some of this light is scattered a few times in the top layer of the sample and is re-emitted to the air. This light maintains most of its initial polarization. A larger percentage of the incident light travels deeper into the sample undergoing multiple scattering before being re-emitted at the surface. This multiple scattering causes the light to become completely unpolarized, see Fig. 2.

In the first measurement when the incident polarizer is set to parallel $\mathbf{I}_{\parallel}^{i}$, the collected light consists of two components. These two components include a parallel component scattered from the top layer of the sample, $\mathbf{I}_{\parallel_{\text{top}}}^{c}$, and 50% of the light that traveled deeper into the sample and lost all its polarization, $\mathbf{I}_{\parallel_{\text{bottom}}}^{c}$. In the second measurement when the incident polarizer is set to perpendicular $\mathbf{I}_{\perp}^{i}$, the light that scatters from the top layer maintains its polarization and is blocked by the analyzer. The perpendicular light that travels deeper into the sample also becomes unpolarized and 50% of the re-emitted light passes through the analyzer as parallel light, $\mathbf{I}_{\parallel_{\text{bottom}}}^{\prime c}$. Thus the first set of collected data includes a small percentage of light from the top layer and a majority of light from the deeper layer, see Fig. 2. The second measure-

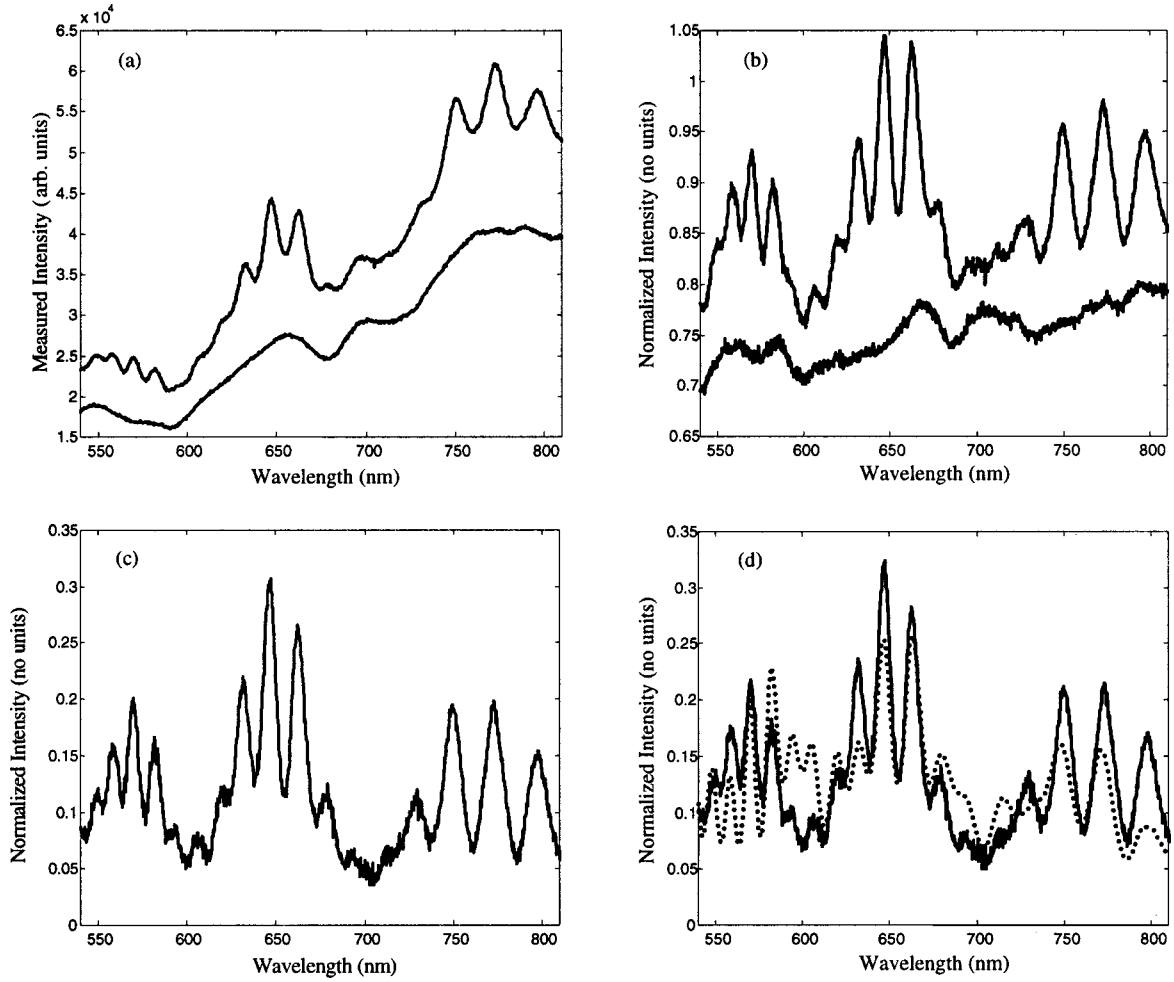

FIG. 3. (a) The measured parallel (top line) and perpendicular (bottom line) intensities collected from the two layer phantom with the 5.8-μm spheres on the top layer with a thickness equal to 84 μm. (b) The same set of data normalized by the diffuser measurements. (c) The parallel measurement minus the perpendicular. (d) The Mie fit (dotted line) to the normalized, subtracted data (solid line).

ment contains no light from the top layer and only multiply scattered light from the bottom layer. By subtracting the second wavelength dependent intensity measurement from the first gives

$$(\mathbf{I}^c_{\parallel_{\text{top}}}+\mathbf{I}^c_{\parallel_{\text{bottom}}})-\mathbf{I}'^{\,c}_{\parallel_{\text{bottom}}}\approx\mathbf{I}^c_{\parallel_{\text{top}}}, \tag{1}$$

where $\mathbf{I}^c_{\parallel_{\text{top}}}$ is the parallel light scattered from the top layer, $\mathbf{I}^c_{\parallel_{\text{bottom}}}$ is 50% of the parallel light scattered from the deep layer, $\mathbf{I}'^{\,c}_{\parallel_{\text{bottom}}}$ is 50% of the perpendicular light scattered from the deep layer. This equation holds true as long as the incident parallel and perpendicular light have equal intensity and the light scattered from the second layer is totally unpolarized. These conditions were approximately met for our experiment as indicated by the good agreement between experiment and theory.

Mie theory provides an exact equation for calculating the intensity of single scattered polarized light from a sphere [15]. This equation is given by

$$\mathbf{I}^s_{\parallel}(\lambda)=[S_2(\theta,\lambda,n_r,x)]^2\mathbf{I}^i_{\parallel}(\lambda), \tag{2}$$

where $\mathbf{I}^s_{\parallel}(\lambda)$ is the scattered intensity, $S_2(\theta,\lambda,n_r,x)$ is an element of the amplitude scattering matrix, θ is the angle between the incident light $\hat{\mathbf{e}}_j$ and the collected light $\hat{\mathbf{e}}_c$, λ is the wavelength of light, n_r is the relative refractive index between the sample medium and a scattering particle, x is the diameter of the particle, and $\mathbf{I}^i_{\parallel}(\lambda)$ is the intensity of incident light. It is worth noting that we only use the parallel scattering amplitude $S_2(\theta,\lambda,n_r,x)$ because we are only fitting light scattered from the top layer. Other components of the light scattered from deeper layers have been removed by subtraction. The incident light is emitted over a solid angle given by $\Delta\theta$ and has the possibility to be scattered by many different sized particles. Summing these combined effects gives the following integral equation:

$$\begin{aligned}\mathbf{I}^s_{\parallel}(\lambda)&=(\mathbf{I}^c_{\parallel_{\text{top}}}+\mathbf{I}^c_{\parallel_{\text{bottom}}})-\mathbf{I}'^{\,c}_{\parallel_{\text{bottom}}}\\&=\mathbf{I}^i_{\parallel}(\lambda)\int_{\Delta\theta}d\theta\int[S_2(\theta,\lambda,n_r,x)]^2f(x)dx,\end{aligned} \tag{3}$$

where $\mathbf{I}^s_{\parallel}(\lambda)$ is equal to the light single scattered from the top layer and $f(x)$ is the PSD. In order to measure $\mathbf{I}^i_{\parallel}(\lambda)$ a sepa-

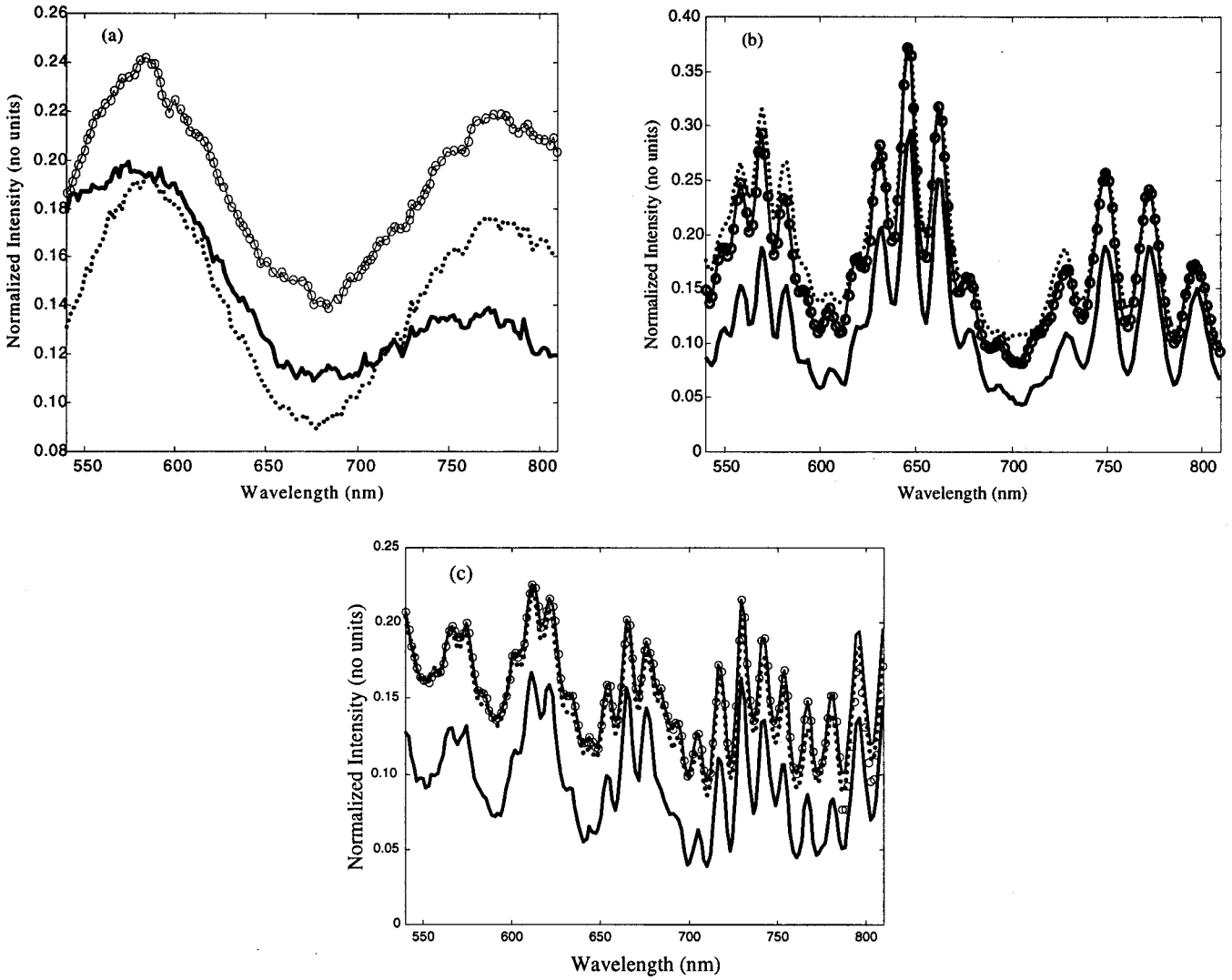

FIG. 4. The measured data from three different thickness. (a) The 0.75-μm spheres with thickness of solid line$=63$ μm, dotted line $=164$ μm, and line with circles$=170$ μm. (b) The 5.83-μm spheres with thickness of solid line$=60$ μm, dotted line$=84$ μm, and line with circles$=179$ μm. (c) The 9.10-μm spheres with thicknesses of solid line$=50$ μm, dotted line$=86$ μm, and line with circles$=121$ μm.

rate set of measurements is made on a standard diffuser. First parallel polarized light is incident onto the diffuser and a measurement is taken. The incident polarizer is rotated so that perpendicular light is incident onto the diffuser and a measurement is taken. Since the diffuser rapidly depolarizes the light and has a very low absorption, the collected diffuser measurements are proportional to the incident intensity, $C\mathbf{I}^{i}_{\parallel}(\lambda)\approx\mathbf{I}^{c}_{\parallel}(\lambda)\approx\mathbf{I}'^{c}_{\parallel}(\lambda)$, where C is a constant. The diffuser measurements also contain the wavelength dependence due to the lenses and polarizers. Thus the wavelength dependence caused by the hardware can be normalized out by dividing $\mathbf{I}^{s}_{\parallel}(\lambda)$ by $\mathbf{I}^{i}_{\parallel}(\lambda)$,

$$\frac{\mathbf{I}^{s}_{\parallel}(\lambda)}{\mathbf{I}^{i}_{\parallel}(\lambda)}=\frac{[\mathbf{I}^{c}_{\parallel}(\lambda)_{\text{top}}+\mathbf{I}^{c}_{\parallel}(\lambda)_{\text{bottom}}]}{\mathbf{I}^{c}_{\parallel}(\lambda)_{\text{diffuser}}}-\frac{\mathbf{I}'^{c}_{\parallel}(\lambda)_{\text{bottom}}}{\mathbf{I}'^{c}_{\parallel}(\lambda)_{\text{diffuser}}}$$

$$\approx C^{-1}\int_{\Delta\theta}d\theta\int[S_2(\theta,\lambda,n_r,x)]^2 f(x)dx, \qquad (4)$$

where $(\mathbf{I}^{c}_{\parallel_{\text{top}}}+\mathbf{I}^{c}_{\parallel_{\text{bottom}}})/\mathbf{I}^{c}_{\parallel_{\text{diffuser}}}$ is the sample's parallel light normalized by the diffuser's parallel light, $\mathbf{I}'^{c}_{\parallel_{\text{bottom}}}/\mathbf{I}'^{c}_{\parallel_{\text{diffuser}}}$ is the parallel component of the sample's perpendicular light normalized by the parallel component of the diffuser's perpendicular light. This normalization using the measurements taken on the diffuser removes any wavelength dependence due to the experimental system.

Since $S_2(\theta,\lambda,n_r,x)$ can be calculated using Mie theory and we use an *a priori* Gaussian distribution for $f(x)$, the right hand side of Eq. (4) can be fit to the measured left hand side of Eq. (4) using a least squared minimization technique. The size distribution of the scattering particles can be determined by fitting the calculated data to the measured data.

IV. RESULTS

Using the fit between our data and the intensity predicted by Mie theory, we were able to extract the PSD of three

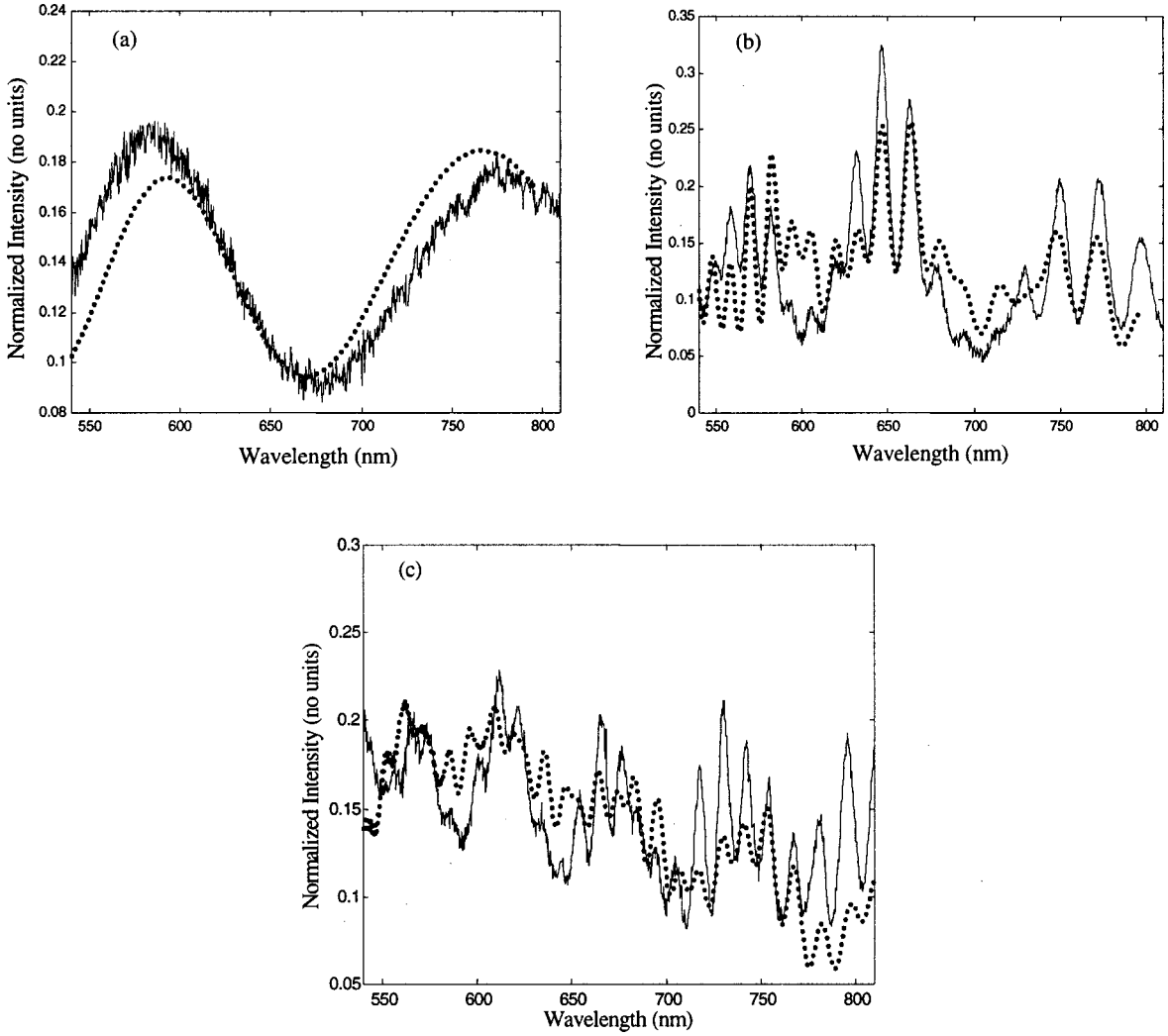

FIG. 5. The measured (solid line) and fitted (dotted line) spectroscopic data for three samples of polystyrene spheres. (a) The measured and fitted data for 0.75-μm spheres with a top layer thickness of 112 μm. (b) The measured and fitted data for 5.83-μm spheres with a top layer thickness of 85 μm. (c) The measured and fitted data for 9.1-μm spheres with a top layer thickness of 86 μm.

different particle mean sizes 0.75, 5.83, and 9.10 μm. For each particle size we took measurements on three different thickness of the sample. We were able to obtain a very reasonable fit between the measured and calculated data for the 0.75 and 5.83-μm particles with the 9.10-μm particle being the most difficult data to match.

In Fig. 3(a) we show the measured intensity collected from the parallel and perpendicular measurements for the 5.83-μm particles. As can be seen in plot (a), the parallel component of the light is significantly higher than the perpendicular component. Both measurements also contain significant wavelength dependence caused by the light source and the polarizers. By normalizing the parallel and perpendicular data by the respective diffuser measurements, the inherent wavelength distortions can be removed, refer to Eq. (4). After normalizing [Fig. 3(b)], the parallel intensity and perpendicular intensity are subtracted [Fig. 3(c)], and then a Mie theory fit of the data is performed, see Fig. 3(d). The oscillations apparent in Fig. 3 are due to the wavelength dependent scattering of the polystyrene spheres in the top layer of the phantom.

For each of the three particle sizes the thickness of the phantom appeared not to affect the measured data. Figures 4(a)–4(c) shows the three data measurements for each sample. There is a significant change in the wavelength dependence of the three diameter spheres, but there is no appreciable difference due to the thickness of the top phantom. The thinnest top layer for the 0.75-μm spheres has a slightly different shape than the thicker measurements. This same trend is not seen for the larger particles where sample thickness should be more critical. Using Mie theory, we were able to fit the measured data to obtain the size distribution of the spheres. Figures 5(a)–5(c) show the measured and fitted data for one of each polystyrene sample.

The reconstructed size distributions are shown in Figs. 6(a)–6(c). In Fig. 6 the normalized size distribution obtained from the polarized measurements is compared to the size distribution obtained by electron microscopy or provided by the manufacturer. The manufacturer's given size distribution, determined by disc centrifuge measurements, was used as the standard for the 0.75-μm latex spheres. However, for the larger samples the manufacturer's size distribution differed

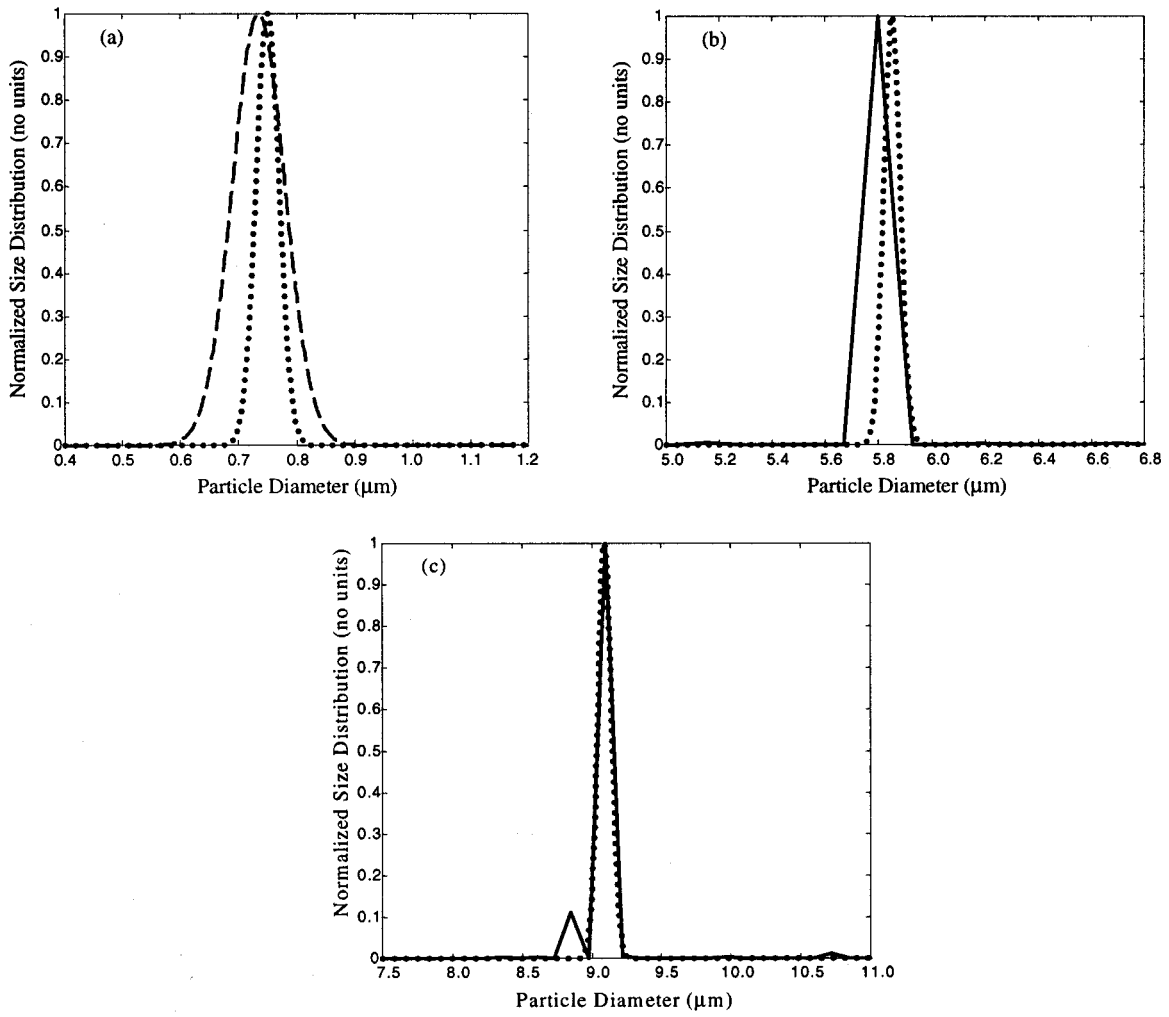

FIG. 6. The normalized size distribution of the three samples. (a) The PSD of the 0.75 μm diameter spheres. The dashed line is the PSD provided by the company compared to the dotted line PSD obtained from our polarized data. (b) The PSD of the 5.8 μm diameter spheres. (c) The PSD of the 9.1 μm diameter spheres. In (b) and (c), the dotted line is the PSD obtained from our polarized data, and the solid line is the PSD obtained from electron microscopy.

significantly from the PSD obtained from the polarized data. We measured the particle sizes of the 5.83- and 9.2-μm spheres directly using electron microscopy. A small drop of each sample was imaged and the number of particles with a particular size counted. The probability size distribution was calculated and normalized for comparison with the polarized measurement. Figures 6(b) and 6(c) show the size distribution measured using electron microscopy, and the reconstructed size distribution from the polarized data. Since the disc centrifuge measurement used by the manufacturer calculated the PSD of a large batch of particles, we believe that the electron microscopy measurements provided more accurate PSD's for our small sample size.

V. DISCUSSION AND CONCLUSIONS

Our experimental setup differed from others because we kept the collection analyzer fixed and rotated the incident polarizer. We used this arrangement because our setup was adapted from a separate study. Although our method should be accurate since $\mathbf{I}_{\parallel}^{i} \approx \mathbf{I}_{\perp}^{i}$, we believe that keeping the incident polarizer fixed while rotating the collection analyzer should be slightly more accurate. The calibration of the system indicated that the incident parallel light was 6% smaller than the perpendicular light. This discrepancy was overcome by normalization.

The other significant difference between this study and other published results is our theory simplification. This simplification is possible since we do not collect directly backscattered light, 180° from the incident. We used a 30° angle between our incident and collection fibers. At this angle there was still a significant percentage of polarized light scattered from the polystyrene spheres for all three samples. The scattering amplitude $S_2(\theta,\lambda,n_r,x)$ was highly dependent upon the angle, and even a 1° shift in the theoretical calculations caused a shift in the reconstructed size distribution. The solid angle range $\Delta\theta$ of the incident light also affected the overall fit of the measured data.

Although the standard deviation provided by the manufacturers is statistically correct, over 95% of the particles are

very near the mean. The large standard deviation arises from a very small number of relatively large particles present in the sample. Apparently, light scattered from these large particles is swamped by light scattered from the much more numerous small particles. This tendency may bode well for using this polarized method on skin where relatively few large scatters such as hairs could potentially affect measurement results.

The sample thickness did not appear to have any quantifiable effect on the intensity spectra or on the reconstructed PSDs. This is a significant result since the epidermal layer also varies in thickness over the body. The ability to reconstruct the PSD of a top layer of polystyrene with thickness of 50 μm without large influence from the Intralipid layer may be due to the strong scattering and absorption of the Intralipid layer. A majority of the light penetrating into the lower layer appears to either be absorbed or loose its polarization because of the high scattering. The dermal layer also has these strong scattering and absorption characteristics due the high concentration of collagen fibers and hemoglobin. These encouraging results lead us to believe that we may be able to distinguish between light scattered from the epidermal layer and the dermis.

This study looked at the feasibility of using polarized light to measure the particle size distribution of three polystyrene samples placed at different thickness on top of a thick bottom layer. Parallel and perpendicular components of linearly polarized light were used to discriminate between light scattered from the top, thin layer of polystyrene and the bottom layer of Intralipid. Mie theory was used to reconstruct the PSD of the top layer by performing a fit of the wavelength dependent scattering intensity. Although the top layer of polystyrene phantom was varied from 50 to 179 μm, the measured data showed almost no dependence on the sample thickness. The reconstructed size distribution produced from this method is in excellent agreement with the distribution obtained from other measurement methods. Our next step will be to improve our experimental setup and measure the cell size distribution of cultured cell samples. Our current study is an important first step toward our ultimate goal to measure the nuclear cell size distribution of skin *in vivo*.

ACKNOWLEDGMENTS

This research was supported in part by a grant from the National Institute of Arthritis and Musculoskeletal and Skin Diseases (NIAMS) (AR46427), a part of National Institutes of Health (NIH).

[1] *Cancer Facts and Figures* (American Cancer Society, Atlanta, GA, 2001).
[2] K. L. McCance and S. E. Huether, *Pathophysiology: The Biologic Basis for Disease in Adults and Children*, 3rd ed. (Mosby, St. Louis, 1998).
[3] R. S. Cotran, V. Kumar, and T. Collins, *Pathologic Basis of Disease* (Saunders, Philadelphia, 1999).
[4] H. Jiang, G. Marquez, and L. Wang, Opt. Lett. **23**, 394 (1998).
[5] M. Bartlett and H. Jiang, AIChE J. **47**, 60 (2001).
[6] S. G. Demos and R. R. Alfano, Appl. Opt. **36**, 150 (1997).
[7] S. L. Jacques, J. Roman, and K. Lee, Lasers Surg. Med. **26**, 119 (2000).
[8] A. H. Hielscher, J. R. Mourant, and I. J. Bigio, Appl. Opt. **36**, 125 (1997).
[9] V. Backman, R. Gurjar, K. Badizadegan, I. Itzkan, R. Dasari, L. Perelman, and L. M. Feld, IEEE J. Sel. Top. Quantum Electron. **5**, 1019 (1999).
[10] M. J. van Gemert, S. L. Jacques, H. J. Sterenborg, and W. M. Star, IEEE Trans. Biomed. Eng. **36**, 1146 (1989).
[11] R. Graaff, A. Dassel, and M. Koelink, Appl. Opt. **32**, 435 (1993).
[12] L. C. Junqueira, J. Carneiro, and R. O. Kelley, *Basic Histology*, 9th ed. (Appleton & Lange, Stamford, CT, 1998).
[13] V. Sankaran, J. T. Walsh, and D. J. Maitland, Opt. Lett. **25**, 239 (2000).
[14] K. M. Yoo and R. R. Alfano, Phys. Lett. A **142**, 531 (1989).
[15] C. F. Bohren and D. R. Huffman, *Absorption and Scattering of Light by Small Particles* (Wiley-Interscience, New York, 1983).